Infrared Cavity Ringdown Spectroscopy of the Water Cluster Bending Vibrations

J. B. Paul, R. A. Provencal, C. Chapo, K. Roth, R. Casaes, and R. J. Saykally*,†

Department of Chemistry, University of California, Berkeley, California 94720

Received: December 4, 1998

We report the first measurement of water monomer bending vibrations in gaseous $(H_2O)_n$ clusters. Infrared cavity ringdown spectroscopy reveals discrete and sequentially blue-shifted bands near 6 μm for $n = 2-4$ and unresolved broad features for $n > 4$, supporting both theoretical predictions and solid-state spectroscopy results. These measurements provide a measure of the monomer distortion that accompanies sequential hydrogen bond formation, which will be valuable for the construction of potential energy surfaces for describing water.

Introduction

Recent experimental and theoretical advances in the study of water clusters are rapidly providing new insight into the nature of solid and liquid water. Most of this effort has involved the measurement and interpretation of terahertz vibration−rotation−tunneling (VRT) spectra, from which details of the intermolecular force fields and hydrogen bond rearrangement dynamics can be extracted. The coupling between inter- and intramolecular modes, as well as the distortion of monomers by polarization effects, is an important complementary feature that can be probed through measurements of the monomer covalent vibrations in the clusters. This was first accomplished in matrix isolation studies,[1,2] but the associated strong environmental perturbations obfuscate the results of these experiments. Vernon and co-workers[3] first measured the O−H stretching spectrum of gaseous water clusters by infrared predissociation measurements near 3 μm. Subsequently, several other groups performed similar indirect measurements, all of which depend on consequences of photon absorption for detection of the spectrum.[4−6] The dynamical processes convolved with the detection process obscure the vibrational transitions themselves, which are most directly probed in an absorption spectroscopy experiment. Such experiments, however, are difficult because of the relatively low sensitivity of direct absorption methods, particularly when used in conjunction with pulsed lasers. We recently reported the first direct absorption results for both the O−H and O−D stretching vibrations of water clusters using our recently developed infrared cavity ringdown technology.[7,8] Here, we report the first measurement of the covalent bending vibrations in gaseous water clusters made by extending the CRLAS technique into the 6 μm region.

Experimental Section

The IR−CRLAS apparatus used to conduct these experiments has been discussed previously.[7,9] Briefly, tunable infrared radiation is generated by Raman shifting a pulsed dye laser (Lambda Physik fl3002e) into the third-Stokes band using a multipass cell containing 200 psi of H_2 gas. The bandwidth of the dye laser was switchable from 0.2 to 0.04 cm^{-1} by installing an intracavity Etalon. After spectral filtering, the laser light is aligned into a two mirror Ringdown cavity. The light leaving the cavity is focused by a 10 cm lens onto an LN$_2$-cooled InSb

detector. The resultant signal is amplified, digitized, and transferred to a PC for real-time fitting to an exponential decay. The determined time-constant is divided into the cavity optical transit time to yield the per-pass fractional cavity intensity loss.

The water clusters were generated in a pulsed supersonic expansion. The helium carrier gas was bubbled through a reservoir of room-temperature water and directed through a 4 in. slit source[10] contained within a Roots pumped vacuum chamber. Various methods were used to systematically adjust the expansion conditions, including altering the source stagnation pressure and limiting the amount of water in the expansion with a needle valve, as discussed below.

Results and Discussion

In contrast with the O−H stretching vibrations, the bending vibrations in water clusters are predicted to exhibit sequential *blue shifts* with increasing cluster size (for the lowest frequency vibrations) accompanied by a *decreasing* per-monomer absorption strength.[11] The hydrogen bonds constrain the motion in the bending coordinate, which accounts for these effects. This translates into a decreased sensitivity to larger clusters, as compared with measurements in the O−H stretch region, along with an increased band congestion, as the vibrational frequencies only spread out by ca. 50 cm^{-1}, rather than the several hundred wavenumber shifts observed for the stretching vibrations.

These theoretically predicted effects are clearly confirmed in the IR−CRLAS spectrum of water clusters in this spectral region, as shown in Figure 1. On the basis of the previous measurements of O−H stretch vibrations, only the absorption bands of the dimer and the trimer should be observable for the lowest concentrations employed here. Additionally, we know that under the present conditions the growth rates of features due to $(H_2O)_2$ through $(H_2O)_4$ with increasing water concentration become sequentially larger with increasing cluster size. Considering these factors, we assign the discrete absorption features appearing at 1600.6, 1613.8, 1614.7, and 1628.6 cm^{-1} to $(H_2O)_2$. The close proximity of the 1600.6 cm^{-1} band to the monomer bend band origin leads to the assignment of this band to the acceptor bend, while the band shape is consistent with that of a parallel transition ($\Delta K = 0$).

The remaining dimer features are assigned to a perpendicular transition ($\Delta K = \pm 1$) involving the donor bending vibration. These presumably correspond to the Q-branches of the A_2 acceptor tunneling component, which carries three times the
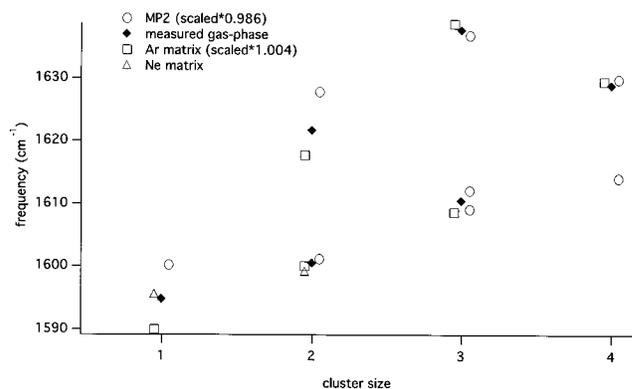
---

† Berkeley Miller Research Professor 1997-98.
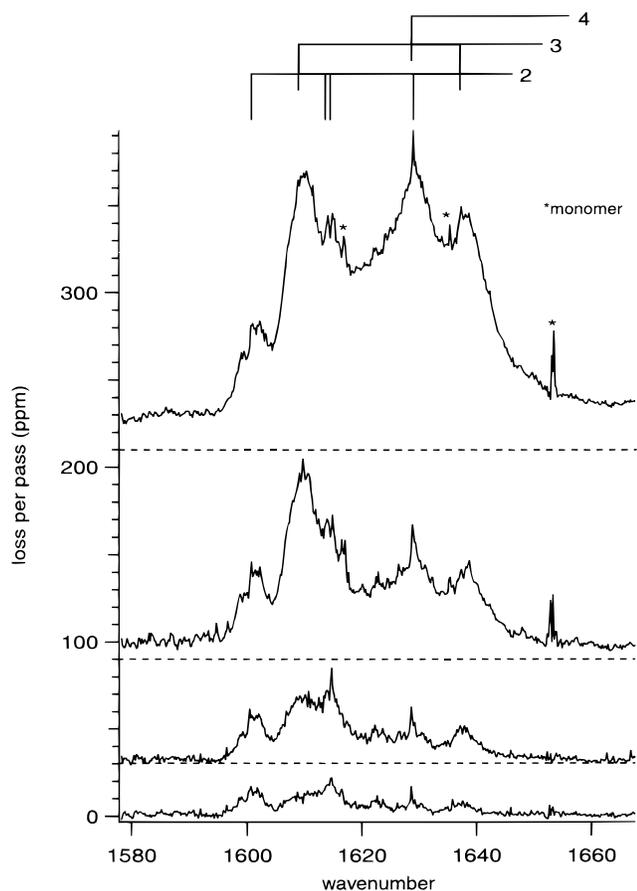
Figure 1. Water cluster spectra in the monomer bending region as a function of increasing water concentration in the expansion. The concentration is varied by seeding a H_2O/helium gas flow into a pure helium flow with a needle valve. The assignments of the discrete features to various sized clusters are given in the upper part of the figure.


Figure 2. Comparison of the measured gas-phase, Ar matrix [ref 2], Ne matrix [ref 12], and ab initio [ref 11] bending frequencies of small water clusters. Note that the Ne matrix results are shown unscaled. (Monomer gas-phase data from ref 12.)

nuclear spin-weight of the A_1 component. Additionally, the Q-branches offer sufficient line density to be observed in the present moderate (1 GHz) resolution study. In contrast, the P and R branches are extremely sparse, and are not easily observed with the present instrument resolution. Because the magnitude of acceptor switching splitting is similar to the $(H_2O)_2$ A rotational constant, the appearance of this band system is expected to be markedly different from that of a "normal" prolate-top perpendicular band, which displays subbands evenly spaced by ca. twice the A rotational constant. Furthermore, since this particular vibrational mode directly influences the hydrogen bond, the upper state tunneling splittings are likely to be significantly changed from those in the ground state. Without additional knowledge of these upper state splittings or of the actual P- and R-branch structure, therefore, the rotational assignment of these bands is not possible at the present time. Likewise, an accurate determination of the band origin is not possible from the present data.

Bands found at 1609 and 1638 cm^{-1} grow dramatically with increasing concentration compared to the $(H_2O)_2$ bands, but they can still be observed at the lowest concentration employed in this study. Therefore, we assign these features to $(H_2O)_3$. At still higher concentration, a distinct band appears centered at 1629 cm^{-1}, which we assign to $(H_2O)_4$. Additionally, a broad, seemingly continuous absorption in the 1600$-$1650 cm^{-1} region must be due to $(H_2O)_4$ and larger clusters. Finally, weak continuum absorption can be seen extending beyond 1650 cm^{-1}, which will be discussed below.

The above small cluster assignments are supported by comparison with results from both cryogenic matrix[12,2] and ab initio studies.[11] The band positions from these studies are plotted along with the present measurements in Figure 2, as a function of cluster size. The previous results have been slightly scaled to provide the best match with the observed gas-phase band locations, with the matrix data requiring a scaling factor of 1.004, while the ab initio results require a factor of 0.986. Once these scaling factors are included, the agreement between the present results with both calculated and argon matrix band positions is excellent. If fact, every major feature observed in the matrix data is reproduced in the gas-phase results, and all of the previous solid-state carrier assignments agree with the present determinations.

While the ab initio $(H_2O)_3$ frequencies[11] compare favorably with the present results, the band intensities do not. Theory predicts that the low frequency feature is actually two bands with a combined intensity of 950 km/mol, whereas the higher frequency band strength is predicted to be only 11 km/mol. These values should be compared with the ca. 2:1 ratio measured in the present study. This discrepancy resembles the differences between the calculated and observed O$-$H stretch band intensities,[13] and certainly warrants further investigation.

We attribute the broad absorption in the 1600$-$1650 cm^{-1} region to water clusters in the $4 < n < 20$ size range, based upon the range of source pressures for which absorption in this region continues to increase. Compared with the O$-$H stretch region, the band density is substantially higher due to the significantly narrower frequency distribution. This, combined with the lower absorption strength of larger clusters, explains why individual features are not readily discerned for clusters larger than $n = 4$ in the present spectra. Additionally, we do not observe a discrete feature for the $(H_2O)_4$ band predicted to lie near 1613 cm^{-1} (Figure 2), presumably for these same reasons.

With conditions favoring the production large clusters (i.e. high water concentration, high source backing pressure) the O$-$H stretching spectrum is dominated by a broad red-shifted "ice-like" feature.[7] The behavior in the bending region is dramatically different, as shown in Figure 3, which compares the weak blue-shifted continuum mentioned above with the absorptions of liquid[14] and amorphous solid[15] water. For reference, the absorption due to the smaller clusters (1600$-$1650 cm^{-1}) extends off the graph at this scale. As was found in the O$-$H region, the spectrum of clusters in this size range of hundreds or even thousands of water molecules per cluster is quite similar to that of the bulk forms of water. The magnitude
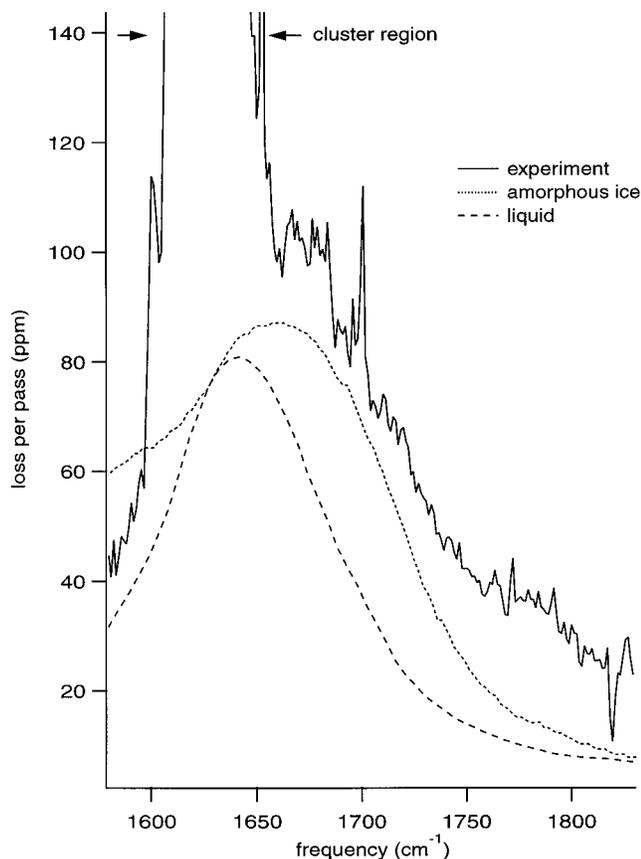
Figure 3. Comparison of the broad absorption feature presently observed with the absorptions of liquid [ref 14] and amorphous solid [ref 15] water.

of the blue shift of this broad feature is indicative of the strength of the hydrogen bonding network. The fact that the gas phase "ice" feature is most blue shifted suggests that the cooperative effects in the hydrogen bond network of clusters in this size range is stronger than those in amorphous ice.

In summary, this work reports a first characterization of the monomer bending vibrations of $(H_2O)_n$ clusters. From these data, we are able to quantify the sequential blue shifts resulting from the cooperative effects in hydrogen bonding. This, in turn, provides a measure of the coupling between inter and intramolecular vibrations, which is essential to elucidate the effects of monomer distortion on the intermolecular potential energy surface.

References and Notes

(1) Brentwood, R. M.; Barnes, A. J.; Orville-Thomas, W. J. *J. Mol. Spectrosc.* **1980**, *84*, 391.

(2) Ayers, G. P.; Pullin, A. D. E. *Spectrochim. Acta* **1976**, *32A*, 1629.

(3) Vernon, M. F.; Krajnovich, D. J.; Kwok, H. S.; Lisy, J. M.; Shen, Y. R.; Lee, Y. T. *J. Chem. Phys.* **1982**, *77*, 47−57.

(4) Coker, D. F.; Miller, R. E.; Watts, R. O. *J. Chem. Phys.* **1985**, *82*, 3554−3562.

(5) Huang, Z. S.; Miller, R. E. *J. Chem. Phys.* **1989**, *91*, 6613−6631.

(6) Huisken, F.; Kaloudis, M.; Kulcke, A. *J. Chem. Phys.* **1996**, *104*, 17−25.

(7) Paul, J. B.; Collier, C. P.; Scherer, J. J.; O'Keefe, A.; Saykally, R. J. *J. Phys. Chem.* **1997**, *101*, 5211−5214.

(8) Paul, J. B.; Provencal, R. A.; Chapo, C.; Pettersson, A.; Saykally, R. J. *J. Chem. Phys.* **1998**. In press.

(9) Paul, J. B.; Provencal, R. A.; Saykally, R. J. *J. Phys. Chem.* **1998**, *102*, 3279−3283.

(10) Liu, K.; Fellers, R. S.; Viant, M. R.; McLaughlin, R. P.; Brown, M. G.; Saykally, R. J. *Rev. Sci. Instrum.* **1996**, *67*, 410−416.

(11) Xantheas, S. S.; Dunning Jr., T. H. *J. Chem. Phys.* **1993**, *99*, 8774−8792.

(12) Forney, D.; Jacox, M. E.; Thompson, W. E. *J. Mol. Spectrosc.* **1993**, *157*, 479−493.

(13) Paul, J. B.; Provencal, R. A.; Chapo, C.; Pettersson, A.; Saykally, R. J. In preparation.

(14) Downing, H. D.; Williams, D. *J. Geophys. Res.* **1975**, *80*, 1656.

(15) Hagen, W.; Tielens, A. G. G. M.; Greenberg, J. M. *Chem. Phys.* **1981**, *56*, 367−379.